AIMS Energy, 11(1): 47–63.
DOI: 10.3934/energy.2023003
Received: 28 August 2022
Revised: 13 January 2023
Accepted: 31 January 2023
Published: 10 February 2023

http://www.aimspress.com/journal/energy

*Research article*

# Performance evaluation of solar still integrated with thermoelectric heat pump system

**Fouad Alkilani*, Ouassini Nemraoui and Fareed Ismail**

Mechanical Engineering Department, Cape Peninsula University of Technology (CPUT), Cape Town, South Africa

*** Correspondence:** Email: fofokelani@ymail.com; Tel: +27610105779.

**Abstract:** This research presents a method for improving a conventional solar still to produce potable water during adverse conditions where there is low or no solar radiation. Summer and winter conditions in the Western Cape province of South Africa were considered. A comparative experimental study was conducted between a conventional solar still and the developed solar still. The developed solar still incorporated a photovoltaic powered thermoelectric heat pump. The purpose of the thermoelectric (TE) heat pump was to accelerate convection inside the developed solar still assembly. The coefficient of performance (COP) of the thermoelectric heat pump installed in the developed solar still ranged from 0.4 to 1.9 at an input current of 5 A. The results indicated that the developed solar still was able to produce 2300 mL per day of drinkable water during a good day in the winter, but the conventional solar still was only able to produce 650 mL per day. The developed solar still produced 2180 mL per day, whereas the ordinary solar still produced 1050 mL per day, during a mild summer day. The developed still had an accumulated water production of 1180 mL during a night with mild temperatures. This significant improvement in yield of the developed solar still system is due to the change in temperature difference between the glazing and the water surface within the developed solar still. This is a significant contribution to the technology of solar water purification.

**Keywords:** solar distillation; solar still; thermoelectric heat pump

**Nomenclature:** A: Area ($m^2$); a: Dependent on the incident angle at the panel; COP: Coefficient of performance; $DT_{max}$: Maximum temperature difference between the cold and hot side of the module;

ED: Electro-dialysis; $f_1$, $f_2$: Circumsolar horizontal incident radiation flux; I: Current (A); $I_{max}$: maximum current (A); $I_T$: Total radiation on the tilted surface (W/m$^2$); $I_b$: Horizontal incident beam flux (W/m$^2$); $I_h$: Total horizontal incident radiation flux; k: Thermal conductivity (W/K); N: Number of thermoelectric junctions; NF: Nano-filtration; MED: Multi effect distillation; $P_{max}$: Maximum tension (kg/cm$^2$); PWM: Pulse Width Modulation; $Q_c$: Heat flow rate at the TE module cold side (W); $Q_{cmax}$: Maximum cooling capacity of the module (W); $Q_h$: Heat release rate at the TEC hot side (W), RO, Reverse osmosis; SD: Solar Distillation; T: Temperature (°C); TE: Thermoelectric; $TE_c$: Thermoelectric cooler; $TE_G$: Thermoelectric generator; $V_{max}$: Maximum voltage (V); VCD: Vapor compression distillation; VD: Vacuum distillation; ZT: Figure of merit

**Greek symbols**: α: Seebeck coefficient (V/k); β: Panel slope; $\rho_g$: Ground reflectivity; σ: Electrical conductivity (S/m)

## 1. Introduction

Water treatment refers to the processing of water to achieve a water quality that meets specified standards set by consumers, communities and organizations through regulatory agencies [1]. Water treatment can be classified into three main methods: chemical, physical and energy-intensive methods [2]. Desalination is the most used approach to produce clean water for drinking, irrigation and industrial purposes. Desalination technologies can be classified into two main categories based on the phase change of the treated water: mechanical and thermal desalination [3]. The first category is desalination without phase change (membrane-based), including reverse osmosis (RO), Nano-filtration (NF) and Electro-dialysis (ED). The second category is desalination that utilizes thermal energy to produce fresh water by evaporation and condensation, including multi-stage flash (MSF), multi effect distillation (MED), vapor compression distillation (VCD), vacuum distillation (VD) and solar distillation (SD) [4,5]. Desalination technologies have become a viable solution for water supply in many coastal countries that have limited natural freshwater resources [6]. A new survey shows that more than 15,900 desalination plants are currently operational, most of them located in the Middle East and North Africa [7]. One of the disadvantages of centralized desalination plants is the intensive energy required to operate the large scale units and to transport the water to the consumers [8]. Moreover, there are negative environmental impacts due to burning fossil fuels, brine disposal and the capital investment cost [9].

Solar distillation is categorized into two main categories: direct solar distillation and indirect solar distillation. In the first category, solar energy is used directly to carry out the evaporation process via devices called solar stills. Meanwhile, in the second category, a solar collector (thermal/photovoltaic) is used as an auxiliary device to provide thermal energy or generate electrical energy to run the distillation unit [10,11]. Direct solar water distillation is similar to the natural hydrological phenomenon of the water cycle; the difference is that solar water distillation is a controlled process (closed-loop system) while the natural water cycle is an open-loop system [12]. Solar distillation technologies are considered a promising alternative over the conventional desalination processes. They have many advantages, such as cost-effectiveness, environmental friendliness and suitability for remote areas where a large-scale desalination facility is not appropriate [13]. However, solar distillation technologies have not been widely used due to the low productivity of potable water. There are two reasons for the low productivity of solar distillation processes. First, the solar still has considerable thermal inertia because of the high specific heat capacity of the contaminated water;

and second, there is difficulty in latent heat rejection of the condensation to the ambient [14]. Therefore, several research studies have been conducted to improve the performance of solar stills. Mohamed et al. [15] investigated the performance of a single-effect solar still equipped with fine stones as a porous absorber with different particle sizes. The results showed that the daily water yield of the solar still increased by 19.8, 27.8 and 33.3% when they used fine stones size of 1 cm, 1.5 cm and 2 cm, respectively. Bataineh and Abo Abbas [16] examined the effect of using both internal reflectors and fins on the performance of a single-slope solar still. They found that the effectiveness of solar stills is improved by installing internal reflectors on three of their sides. The efficiency increased by 36 and 47% in January and December, respectively. Porta-Gándara et al. [17] investigated the increase in water output of a 1.7 $m^2$ single-slope solar still equipped with a perturbation device. Through this apparatus, air bubbles are injected into the water basin, which results in ripples on the water's surface. This results in an increase in the overall evaporative surface area and stimulates the mass transfer coefficient. The results showed that on a sunny day, the daily distillation production was 6.1 kg in a semi-desert region of La Paz, Mexico. Jani and Modi [18] examined the impact of cavity fins on the performance of a double slope solar still. The results indicated that the optimal water depth for desalination was 1 cm and that circular fins performed better than fins with a rectangular cross-section. The maximum water yield produced from the circular finned solar still was 1.49 kg/$m^2$-day, while the square finned solar still produced 0.96 kg/$m^2$-day. Kabeel and Abdelgaied [19] studied the performance of pyramidal solar still equipped with graphite absorber plate that had a high thermal conductivity as well as cooling of the condensation surface. The results indicated that combining the two methods could increase distillation efficiency by 97.2–98.9% compared with a conventional pyramid still. Esfe et al. [20] presented a mathematical model to study the effect of the dimensions of a solar still equipped with thermoelectric system. The obtained results showed that the water yield improved by 6.8% compared to the conventional solar still. Esfe and Toghraie [21] introduced a numerical method to investigate the performance of a solar still with thermoelectric cooling system. The results showed that the use of the thermoelectric cooling system improved the daily water yield by 62% under the weather of Semnan province of Iran. Sheikholeslami et al. [22] introduced numerical simulation for thermal analysis of a parabolic solar collector with wavy absorber pipe and nanofluid. The results showed a 180% improvement in heat transfer coefficient. In addition, the performance and categorization of solar stills based on design guidelines, efficiencies and productivity were investigated by [14,23–28].

As noted in the literature review, most of these related studies on solar still performance enhancement focused on the productivity improvement by changing the design, structure or operation parameters. These kinds of improvements may work on ideal days (sunny, warm days). Note that, however, solar still systems still show poor performance on cloudy and partly cloudy days. Moreover, during hot days, the pure water yield decreases due to the low water-cover temperature difference. With this research gap identified, this work has therefore been undertaken to effectively improve the efficiency of a conventional solar still by employing a thermal energy backup system. A solar photovoltaic powered thermoelectric heat pump system is designed and integrated with the conventional solar still. Seasonal performance of the advanced solar still is reported in the research work herein with respect to the overall energy efficiency. The article is organized as follows: A literature review with focus on the water crisis and the attempted solutions is presented. Then, the principle of a solar still with emphasis on the developed solar still is presented, followed by practical

designs and implementations of the developed and conventional solar stills. The experimental results are analyzed and compared, with the conventional solar still as the reference. Important findings are noted, concluding remarks are made, and recommendations are made for further studies.

## 2. Overview of the thermoelectric heat pump system

The thermoelectric phenomenon is the conversion of thermal energy into electrical energy or vice versa [29]. The conversion of electric energy into a temperature gradient is called the Peltier effect, while the reverse phenomenon is called the Seebeck effect [30]. Since the advent of semiconductor materials, thermoelectric devices ($TE_C/TE_G$) have become widely used in many fields, such as building ventilation and air conditioning [31], the automotive industry [32], waste heat recovery [33] electronic equipment cooling [34].

As a solid state heat pump, thermoelectric devices have many advantages over conventional heat pump systems, such as compact size, no moving parts, environmental friendliness due to the lack of use of refrigerants and fast convenient heating and cooling sustainability. The coefficient of performance of thermoelectric heat pumps is relatively low compared with conventional systems. The trend of low performance is mainly caused by the poor heat conversion efficiency of the semiconductor materials, which is reflected by the figure of merit (ZT) value [35]. The value of figure of merit can be derived from Eq (1).

$$\mathrm{ZT} = \frac{\alpha^2 \sigma}{\mathrm{k}} \mathrm{T} \tag{1}$$

where α is the Seebeck coefficient ($VK^{-1}$), σ is the electrical conductivity (S/m), k is the thermal conductivity (W/K), and T is the absolute temperature. The coefficient of performance (COP) of the thermoelectric heat pump can be defined as in Eq (2).

$$\mathrm{COP} = \mathrm{Q_h}/(\mathrm{Q_h} - \mathrm{Q_c}) \tag{2}$$

$$Q_h = \alpha_m I T_h - K_m (T_h - T_c) + \frac{1}{2} R_m I^2 \tag{3}$$

$$Q_c = \alpha_m I T_c - K_m (T_h - T_c) - \frac{1}{2} R_m I^2 \tag{4}$$

where $Q_h$ is the flow of heat to the heat sink (heating capacity), $Q_c$ is the flow of heat from the heat source (cooling capacity), $I$ is the applied current, $T_h$ is the temperature of the hot side of the module, $T_c$ is the temperature of the cold side of the module, and $R_m$ is the electric resistance. The properties α, σ and $k$ are essential to determine the performance of thermoelectric materials. The specifications of the modules used in this research are listed in Table 1.

**Table 1.** TEC1-12706 specifications.

| Type | $I_{max}$ | $V_{max}$ | Couples *(N)* | $QC_{max}$ (W) | $DT_{max}$ (ºC) | *R* (Ω) | *K* (W/K) | $P_{max}$ (kg/cm$^2$) | Dimensions (mm) |
|---|---|---|---|---|---|---|---|---|---|
| TEC1-12706 | 6 | 15 | 127 | 65 | 70–80 | 1.53 | 0.5 | 10.8 | 40*40*4 |

## 3. Materials and methods

Figure 1 shows a photograph of the experimental apparatus of the developed solar still proposed in this research, which basically consists of a single-effect basin type solar still integrated with a thermoelectric heat pump system. The basin section is made of 0.5 $m^2$ aluminum sheet. A polystyrene board with a thickness of 15 mm was used as a thermal insulator. It is sandwiched between the aluminum sheets of each side of the solar still. The basin liner was coated in black using waterproof and high heat resistant paint to maximize solar energy absorptivity. A polycarbonate sheet with a thickness of 1 mm was used to cover the basin. Thermal silicon was used to seal the edges. The thermoelectric heat pump system section consists of six $TE_C$ modules, two water-cooled heat sinks, two 10 W DC water pumps, circuit controls and a plumbing system. The heat sinks are made of aluminum tanks. Thermal grease was applied to attach the thermoelectric modules to the heat sinks. Insulation cotton washers designed specifically for $TH_C$ application were used to prevent moisture formation around and inside the TE module. Typical fasteners were used to mount the arrangement, and 15 $kg/cm^2$ is the recommended tension to maintain proper contact with the TE heat sinks assembly. The cold side of the heat pump was connected to the cold water inlet of the condensation surface, while the hot side was connected to the heat exchanger routed inside the basin. A PV system consisting of a 270 W PV panel, circuit breaker, 20 A pulse width modulation (PWM) charge controller and 200 Ah deep cycle battery was used to power the thermoelectric heat pump system.

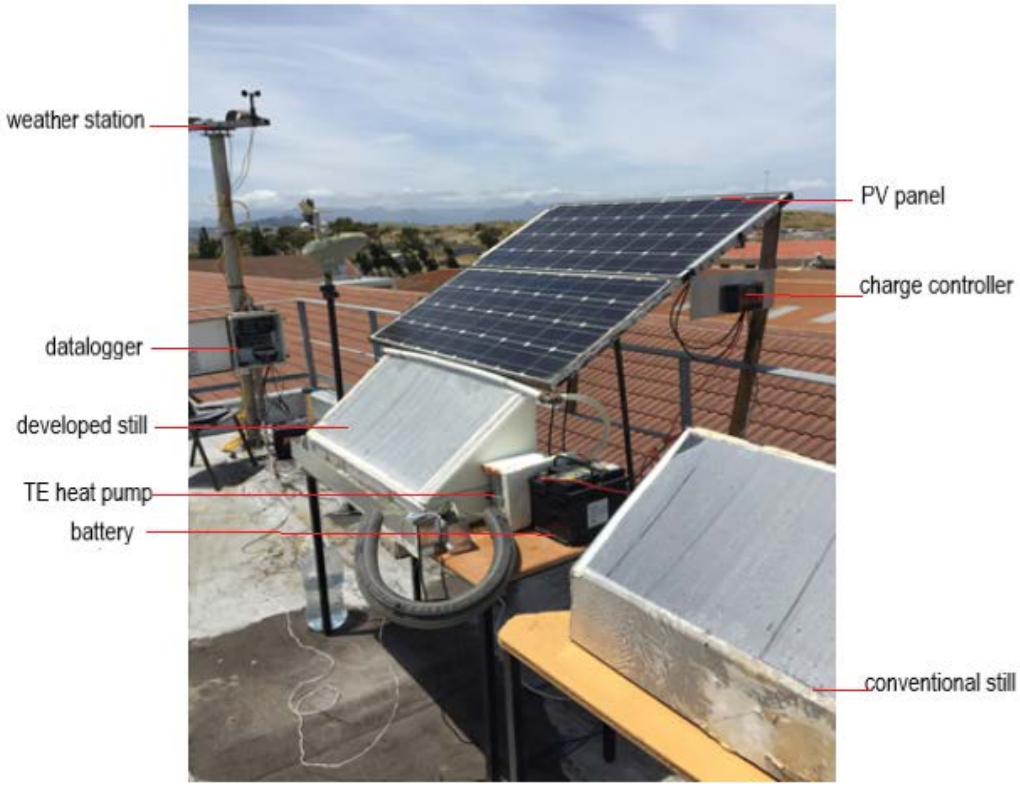


**Figure 1.** Pictorial view of the experiment apparatus.

The experiment was conducted outdoors to evaluate the system performance under different weather conditions. Its site is located at 33.92° S, 18.4° E. Elevation was about 68.5 m above sea level. The selected tilt angle of both collectors (PV & still cover) was about 35.5°. In addition, an identical conventional solar still was used for comparison with the developed one. A set of thermocouples was used to measure the temperature of the water inside the basin, the condensation surface and other components of the TE heat pump system. Figure 2 shows a schematic diagram of the developed solar still and the positions of the thermocouples. A data logger meteorological station equipped with two pyranometers and an anemometer was used to record the incident solar radiation and wind velocity.

The basins in both stills were filled with 10 L of seawater. The desirable water depth is about 20–30 mm [36]. For the developed solar still, it is crucial to keep the heat exchanger always submerged.

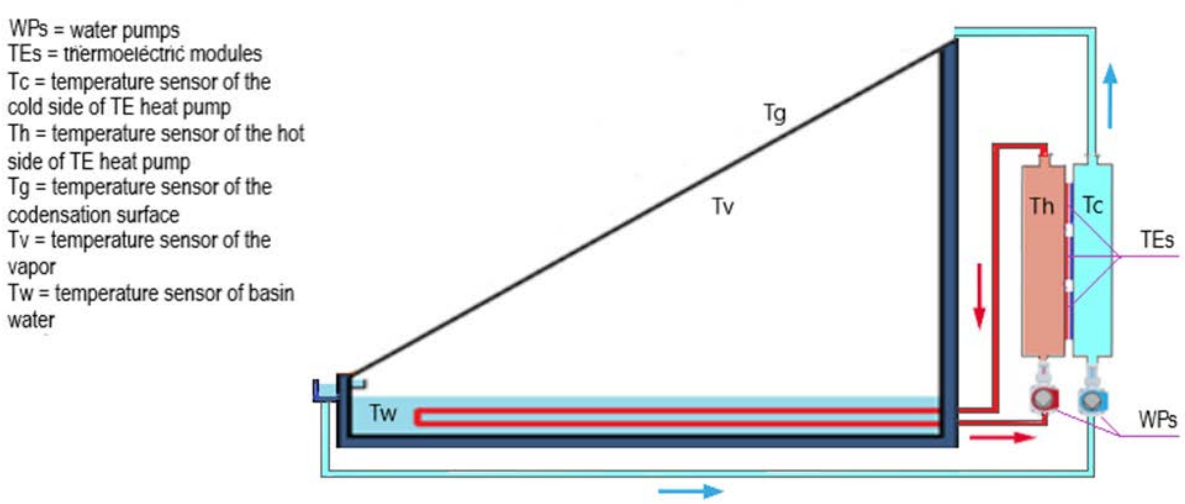


**Figure 2.** Schematic diagram of the developed solar still.

## 4. Results and discussion

This section presents and discusses the experimental results of the outdoor experimental test conducted to evaluate the performance of the conventional single-effect solar still integrated with thermoelectric heat pump system. A comparison between the conventional solar still and the developed solar still is discussed from a thermodynamic point of view.

### *4.1. The meteorological conditions of the test location*

During the experimentation period, the weather conditions of the location of the experiment were monitored using a weather station mounted at the top of the university's mechanical engineering building. Samples of the weather conditions over the course of the testing period are illustrated in Figures 3,4. During a typical summer day, the ambient temperature can reach up to 35 °C, while on a winter day, the ambient temperature average is around 15 °C. The wind

speed has seasonal dependence, and it ranges between 0.5 and 14.7 m/s.

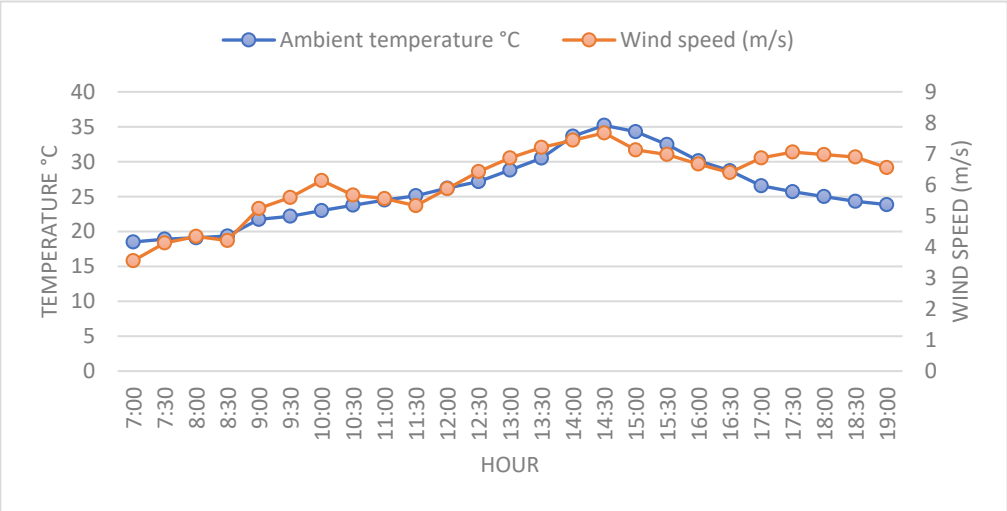


**Figure 3.** The variation of wind speed and ambient temperature during a typical summer day (2021).

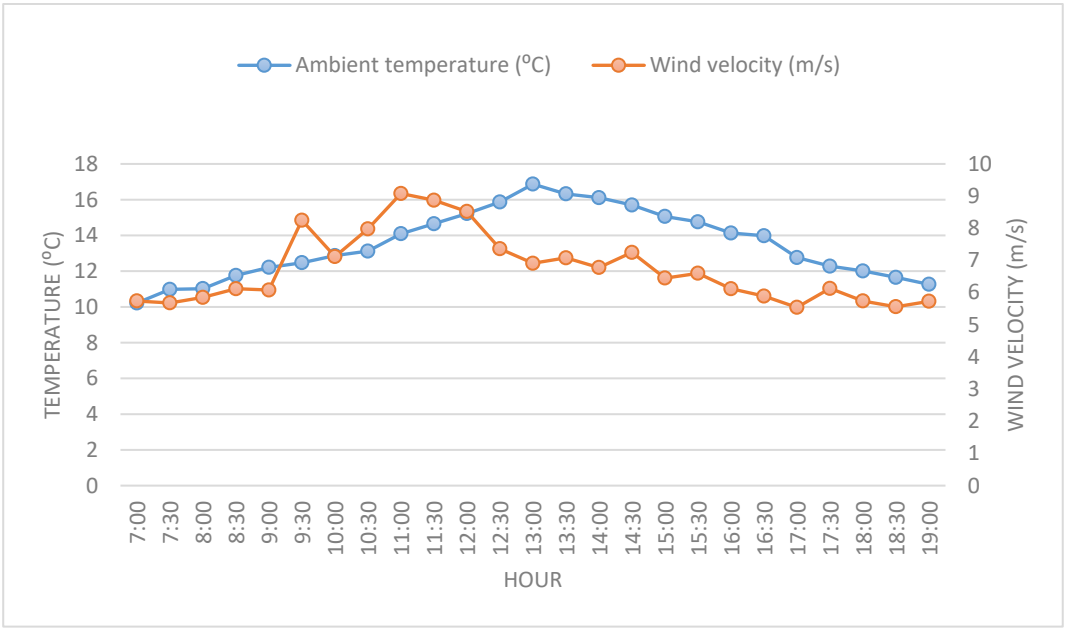


**Figure 4.** The variation of wind speed and ambient temperature during a typical winter day (2021).

Figure 5 shows the variation of the computed incident solar radiation on the solar collectors (PV and solar still). The value of the solar radiation on the tilted surface was calculated by using the Perez formula (Eq 5).

$$I_T = I_b R_b + I_d \left[(1 - f_1)\left(\frac{1+\cos\beta}{2}\right) + F_1 \frac{a}{b} + F_2 \sin\beta\right] + I_h \rho_g \left(\frac{1-\cos\beta}{2}\right) \quad (5)$$

As shown in the graphs, the maximum solar radiation recorded during a week of the experimental test in May 2021 was 827 W/m$^2$. Day 5 shows a fluctuation in incident solar radiation

due to a partly cloudy sky.

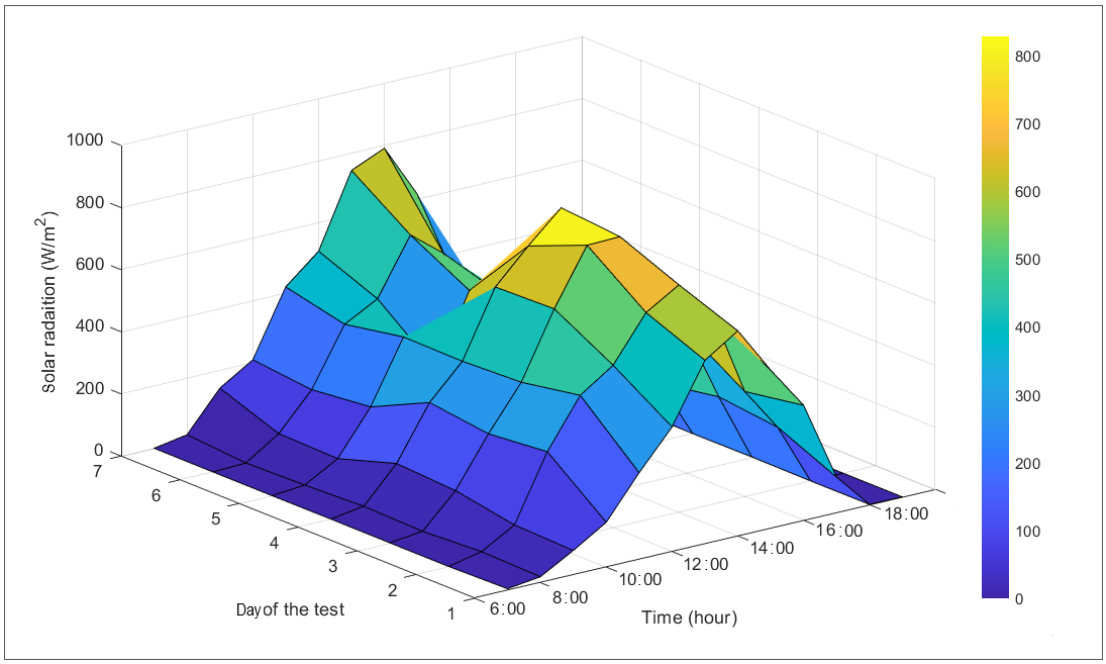


**Figure 5.** The variation of incident solar radiation in May 2021.

Figure 6 shows the trend of the incident solar radiation in the early days of September 2021, and the maximum value of the computed solar radiation during six experimental days was 680 W/m$^2$. On a mostly cloudy day, the maximum value was 135 W/m$^2$.

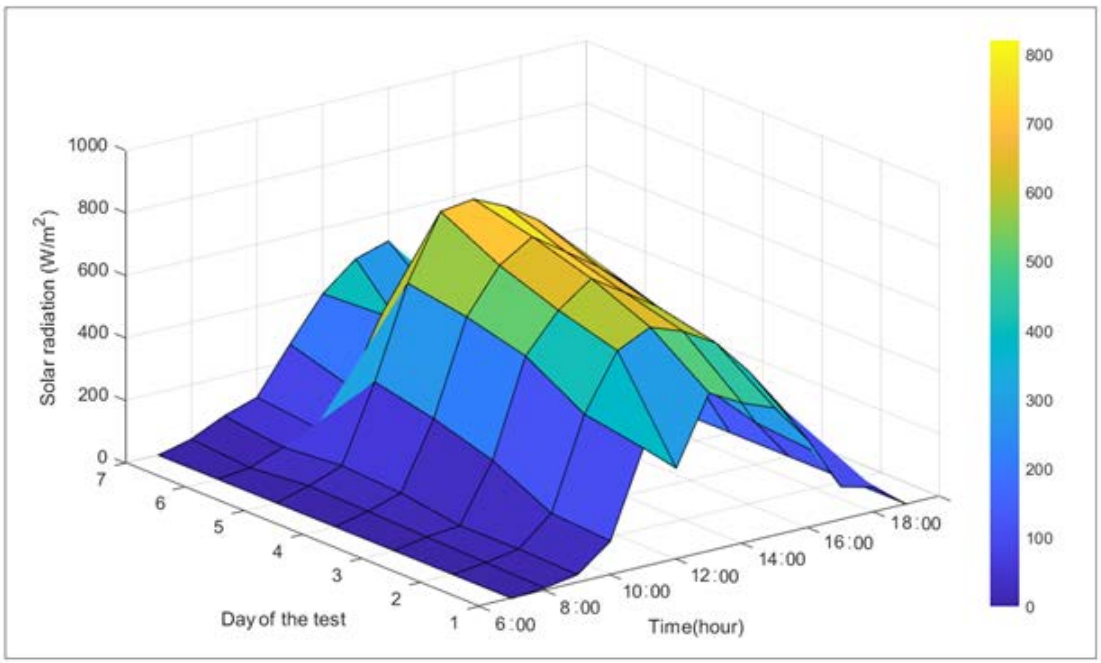


**Figure 6.** The variation of incident solar radiation in September 2021.

*4.2. The developed and conventional solar stills' performances*

The water to water thermoelectric heat pump consists of 6 TEC-12706 modules integrated into a single-effect solar still to enhance the daily potable water productivity. An identical conventional solar still was used as a reference to evaluate the performance. The stills were operated simultaneously side by side. The temperatures of both solar stills' components were monitored. Herein, $T_w$ represents basin water temperature, $T_v$ represents vapor temperature, $T_g$ represents condensation surface temperature, and $T_a$ represents ambient temperature.

The distillate yields of both stills were recorded. Also, the effect of the temperature difference between the cold and hot sides of the module on the coefficient of performance (COP) of the thermoelectric heat pump system was investigated.

Figure 7 presents the temperature trend of the developed solar still's components. The ambient temperature recorded at the start of the experiment was 17 °C, and it then increased to 26 °C at midday. The initial temperature of the water basin was 16 °C, and it then increased to 45 °C within 4 hours. At midday, the basin water temperature reached 60 °C. It stayed above 50 °C till 17:00 and then decreased to 49 °C at the end of the experiment. The sharp increase in basin water temperature was due to the input heat delivered from the TE heat pump system. The vapor temperature had the same trend as the basin water temperature. It reached 54 °C at midday. The temperature difference between the water basin and the condensation surfaces is the key aspect of the solar still. It stayed above 20 °C. The highest value recorded was 32 °C.

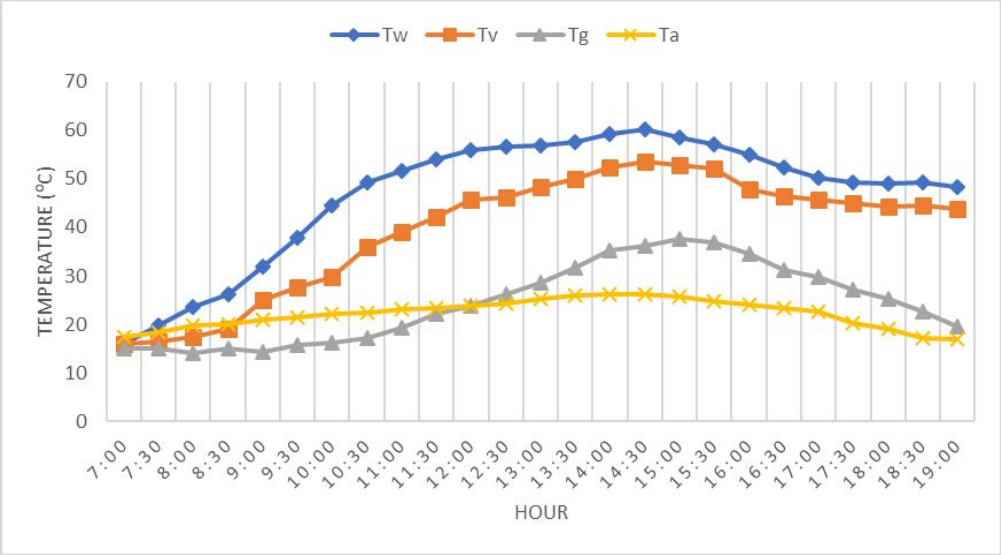


**Figure 7.** The temperature trend of the developed solar still.

Figure 8 presents the temperature trend of the conventional solar still. The ambient temperature recorded at the start of the experiment was 17 °C, and then increased to 26 °C at midday. At the end of the experiment, the ambient temperature decreased to 18 °C. The initial temperature of the water basin was 16 °C, and within 3.5 hours, it reached 26 °C. There was a linear increase in the water basin temperature until midday, after which a linear decreasing tendency was noticed. The maximum basin temperature recorded was 53 °C. The vapor temperature had similar behavior as the water basin temperature. It reached 49 °C at midday. The condensation surface temperature increased with

the increase of the vapor temperature. The maximum value recorded was 41 °C at midday. The temperature difference between the water basin and the condensation surfaces varied between 4 and 14 °C.

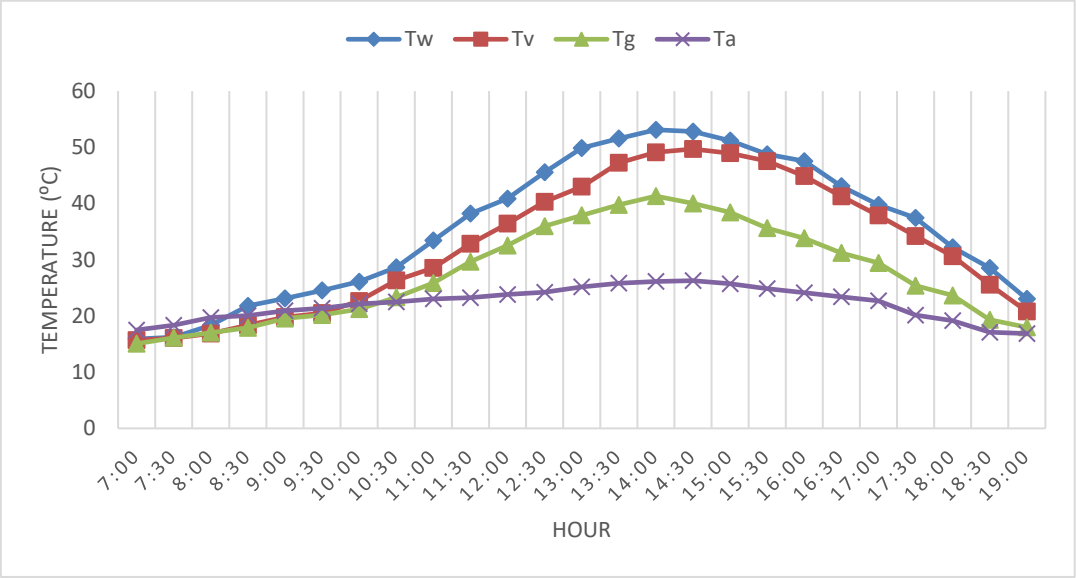


**Figure 8.** The temperature trend of the conventional solar still.

Figure 9 depicts the yields of water distillates of both solar stills. As can be observed from the graph, the water yield from the developed still started early, at 8:30, while the conventional still produced water at 10:30. The highest amounts of distillate for the developed and conventional stills were collected at 14:30 and 15:00, respectively. The incident solar radiation was 660 W/m$^2$. The accumulated water distillate at the end of the experiment was 2180 mL (4.4 L/m$^2$) for the developed still, while the conventional still produced 1050 mL (2.1 L/m$^2$).

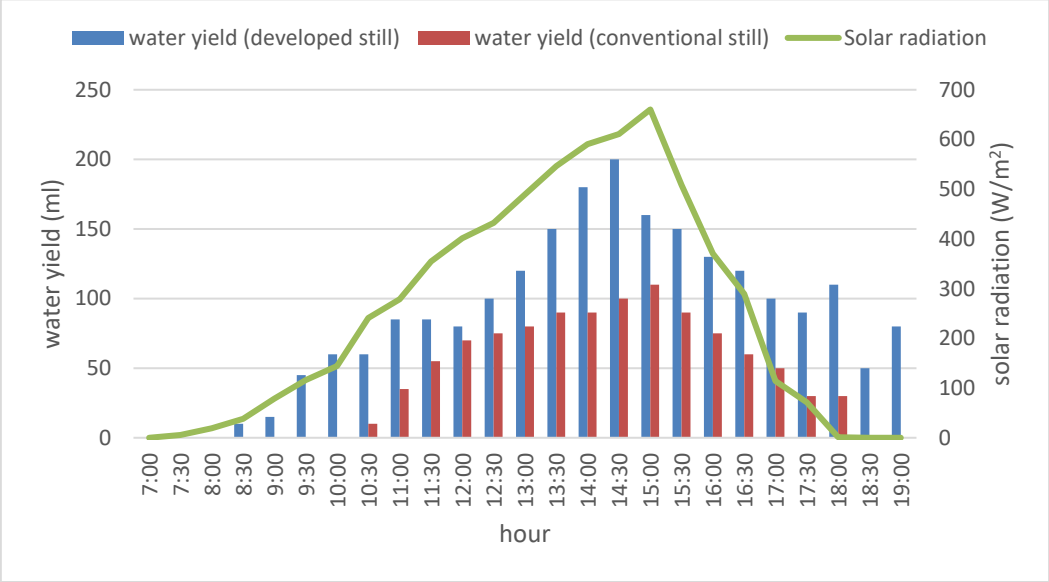


**Figure 9.** The accumulated water yields from solar stills in May 2021.

The performance of the developed solar still in September 2021 is presented in Figure 10. As is noticeable in the graph, the condensation surface temperature increased gradually after 12:00, due to the fact that the thermoelectric pump was off until 15:30, since the water basin temperature stayed above 52 °C. The maximum water basin temperature recorded was 54.8 °C at 14:00, and the maximum ambient temperature was about 17.7 °C at midday. The average temperature difference between the water basin and the condensation surfaces was 24 °C.

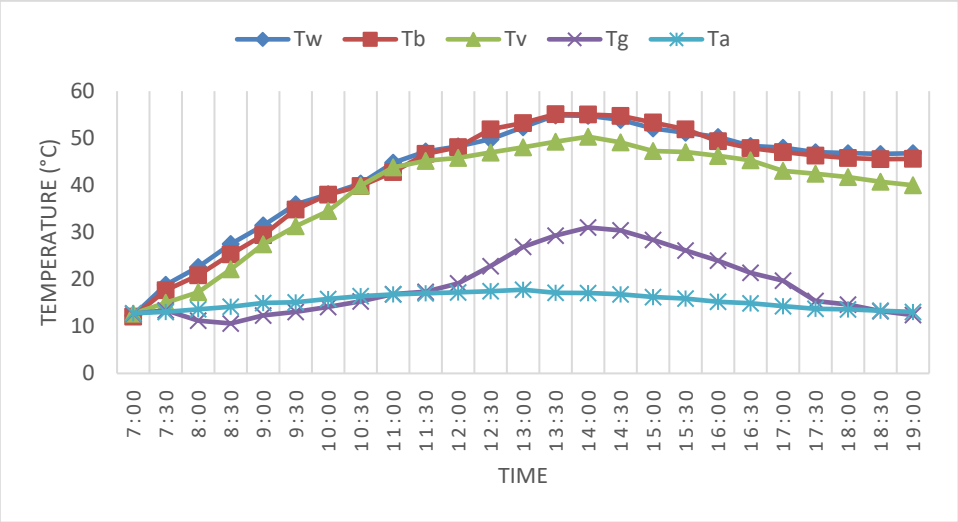


**Figure 10.** The temperature trend of the developed solar still in September 2021.

Figure 11 depicts the temperature trends in the conventional solar still components. The highest temperature of the water basin, recorded at 13:30, was 45.8 °C. Because of the low intensity of solar radiation, the water basin temperature remained relatively low throughout the day. The average of the temperature difference between the water basin and the condensation surfaces was 11 °C

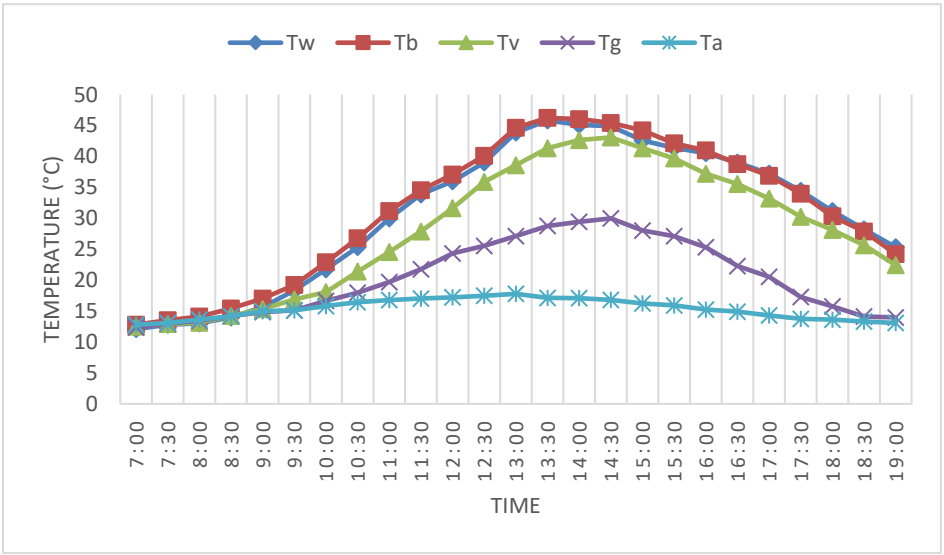


**Figure 11.** The temperature trend of the developed solar still on September 2021.

Figure 12 depicts the accumulated distillate water of both solar stills. As can be observed from the graph, the water yield from the developed still started early, at 9:30, while the conventional still produced water at 11:00. The highest amounts of distillate for the developed and conventional stills were collected at 14:30 and between 13:30 and 14:30, respectively. The incident solar radiation was 530 W/m$^2$. The ambient temperature was relatively low, and the highest value recorded at 13:00 was 17.8 °C. The accumulated distillate water at the end of the experiment was 4.6 L/m$^2$ for the developed still, while the conventional still produced 1.3 L/m$^2$.

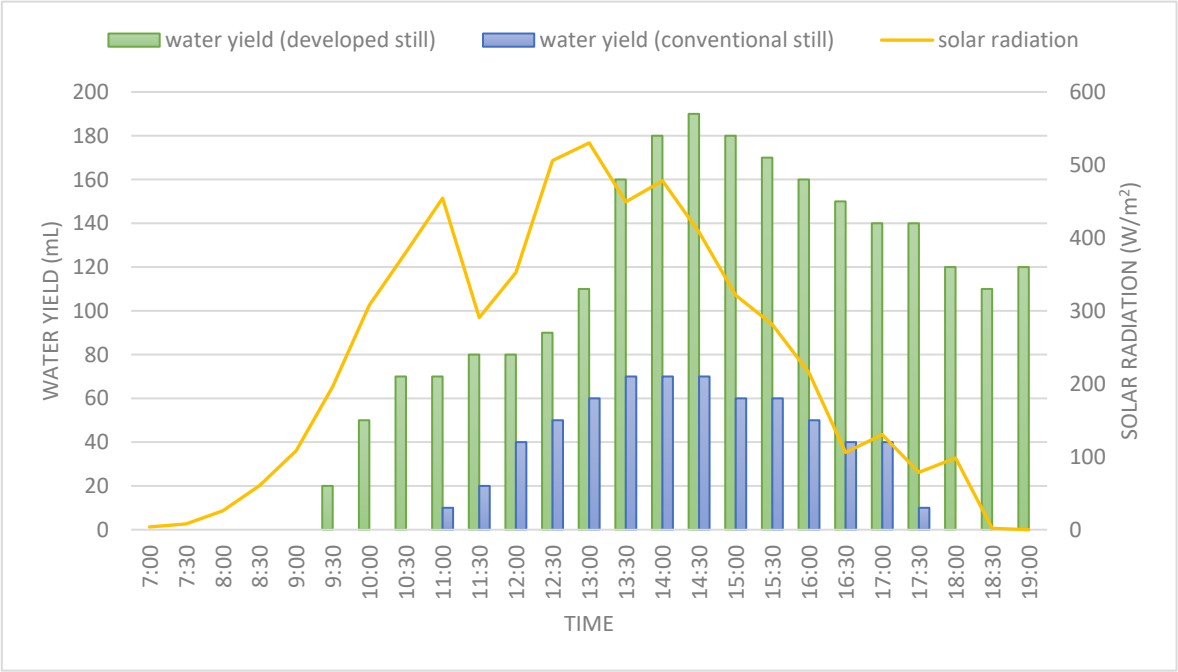


**Figure 12.** The accumulated water yields from solar stills in September 2021.

The performance of the developed still during a relatively cold night in September 2021 is shown in Figure 13. The water basin temperature ($T_w$) reached 43 °C at 23:00. The highest value recorded was 50.4 °C. The thermoelectric heat pump system was able to maintain the temperature at around 49 °C until the end of the experiment. The ambient temperature varied between 11.4 and 16.4 °C. The average temperature difference between the water basin and the condensation surfaces was 27 °C. As observed from the graph, the condensation (water yield) began at 22:00. The accumulated water yield at the end of the test was 1180 mL (2.360 L/m$^2$).

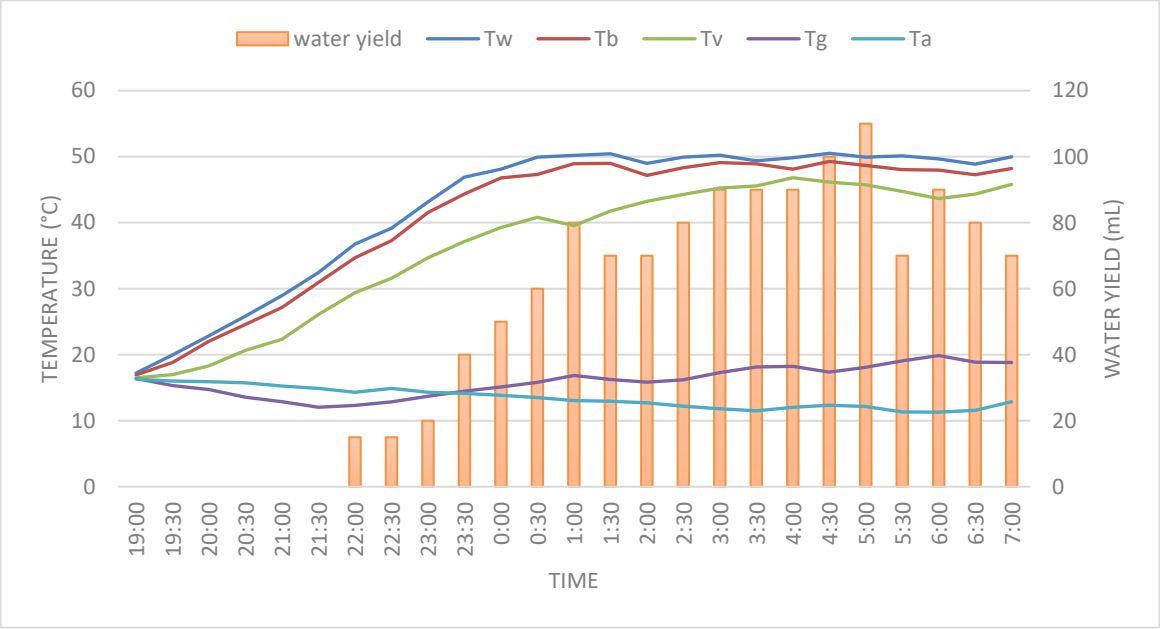


**Figure 13.** The developed solar still performance at night (September 2021).

Figure 14 shows the variation of the coefficient of performance of the heat pump system at the input current of 5 A. It is noticeable that the COP declines with the increase of the cold side temperature of the thermoelectric modules ($T_c$). At 8:00, the temperature of the cold side of the thermoelectric module was 10 °C, the hot side was 28 °C, and the value of the COP was 1.9. At 14:00, the temperature of the cold side increased to 29 °C, and the value of the COP decreased to 0.4 due to the increase in the cooling capacity ($Q_c$). At the end of the experiment (19:00), the value of the COP increased again due to the decrease of $T_C$, which was 13 °C. These findings are in agreement with the results found by [37].

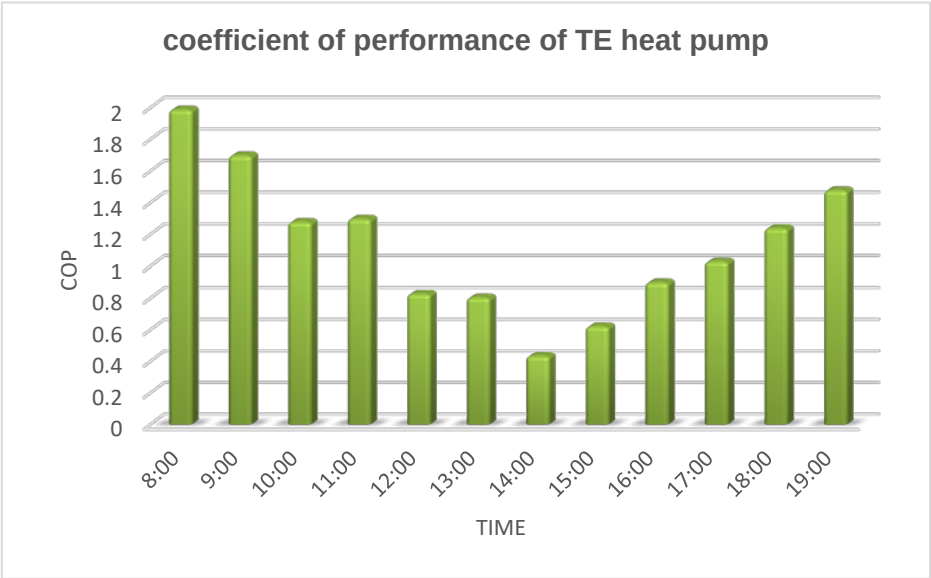


**Figure 14.** The variation of the coefficient of performance of the TE heat pump system.

## 5. Conclusions

This research work investigated the performance of a thermoelectric water-to-water heat pump system integrated into a conventional solar distillation unit. A typical solar photovoltaic system was designed to power the thermoelectric heat pump components. The main benefit of the integrated thermoelectric heat pump is that it increased the daily yield of fresh water by means of heating up the saline/brackish water and cooling down the condensation surface, thus increasing the temperature difference between the water basin and the condensation surfaces. This is considered the key factor of the solar still operation. Summer and winter outdoor experiments were conducted to investigate the performance of the solar still under different weather conditions. The obtained results are summarized as follows:

- The results of the summer outdoor experiments showed that at an incident solar radiation of 660 W/m$^2$ and an ambient temperature of 26 °C, the maximum water basin temperature of the developed solar still was 60 °C, and the daily distillate yield was 2180 mL (4.4 L/m$^2$). Meanwhile, the maximum basin water temperature recorded for the conventional solar still was 53 °C, and the water yield was 1050 mL (2.1 L/m$^2$).
- On a moderate winter day, the accumulated water yield was 2300 mL (4.6 L/m$^2$), and the maximum water temperature was 54 °C. Despite the low average of the incident solar radiation and low ambient temperature, the daily yield was satisfactory due to the higher temperature difference between the water and the condensation surfaces, which was evaluated as 35 °C. Meanwhile, the accumulated water yield from the conventional still was 650 mL (1.3 L/m$^2$). The maximum basin water temperature achieved was 46 °C.
- The results for the developed still during a moderate night in the month of September 2021 showed that the highest water basin temperature was 50 °C, and the accumulated distillate yield was 1180 mL (2.36 L/m$^2$).
- The maximum value of COP of the thermoelectric heat pump according to energy balance equations and the principles of thermodynamics for a single-stage heat pump was about 1.9.

Based on this work, the integration of the thermoelectric heat pump system into a conventional solar still has shown significant improvement of the daily fresh water productivity. The thermoelectric heat pump system can be integrated into different types of passive solar stills. Herein, simple modifications may be required for the thermoelectric heat pump layout to match the different designs of the solar stills.

For future work, more investigations are needed to improve the thermoelectric heat pump performance. Therefore, the authors recommend further exploration of the use of other types of thermoelectric modules. Moreover, cascades or multi-stage cycles can be addressed in further studies.

## Conflict of interest

There is no conflict of interest. This research did not receive any specific grant from funding agencies in the public, commercial or not-for-profit sectors.

## Author contributions

Fouad M Alkilani performed Conceptualization, Methodology, Writing, Original draft preparation and editing.

Dr. Ouassini Nemraoui performed Supervision and Reviewing.
Dr. Fareed Ismail performed Supervision and Reviewing.

## References


1. Liang R, Hu A, Hatat-Fraile M, et al. (2014) Fundamentals on adsorption, membrane filtration, and advanced oxidation processes for water treatment. In: *Nanotechnology for Water Treatment and Purification*, Knoxville, Springer, 1–45. https://doi.org/10.1007/978-3-319-06578-6_1
2. Cheremisinoff NP (2002) Handbook of Water and Wastewater Treatment Technologies, 1st ed., Woburn—USA: Butterworth-Heinemann, 2002. https://doi.org/10.1016/B978-075067498-0/50004-8
3. Bundschuh J, Kaczmarczyk M, Ghaffour N, et al. (2021) State-of-the-art of renewable energy sources used in water desalination: Present and future prospects. *Desalination* 508: 115035. https://doi.org/10.1016/j.desal.2021.115035
4. Misdan N, Lau WJ, Ismail AF (2012) Seawater Reverse Osmosis (SWRO) desalination by thin-film composite membrane—Current development, challenges and future prospects. *Desalination*: 228–237. https://doi.org/10.1016/j.desal.2011.11.001
5. Darre NC, Toor GS (2018) Desalination of water: A review. *Curr Pollut Rep* 4: 104–111. https://doi.org/10.1007/s40726-018-0085-9
6. Elsaid K, Kamil M, Sayed ET, et al. (2020) Environmental impact of desalination technologies: A review. *Sci Total Environ* 748: 141528. https://doi.org/10.1016/j.scitotenv.2020.141528
7. Jones E, Qadir M, van Vliet, et al. (2019) The state of desalination and brine production: A global outlook. *Sci Total Environ* 657: 1343–1356. https://doi.org/10.1016/j.scitotenv.2018.12.076
8. Shahabi MP, McHugh A, Anda M, et al. (2017) A framework for planning sustainable seawater desalination water supply. *Sci Total Environ* 575: 826–835. https://doi.org/10.1016/j.scitotenv.2016.09.136
9. Lattemann S, Höpner T (2008) Environmental impact and impact assessment of seawater desalination. *Desalination* 220: 1–15. https://doi.org/10.1016/j.desal.2007.03.009
10. Zhang Y, Sivakumar M, Yang S, et al. (2018) Application of solar energy in water treatment processes: A review. *Desalination* 428: 116–145. https://doi.org/10.1016/j.desal.2017.11.020
11. Huang W, Su P, Cao Y, et al. (2020) Three-dimensional hierarchical CuxS-based evaporator for high-efficiency multifunctional solar distillation. *Nano Energy* 69: 104465. https://doi.org/10.1016/j.nanoen.2020.104465
12. Tiwari GN, Sahota L (2017) Advanced solar-distillation systems: basic principles, thermal modeling, and its application. *Springer*. Available from: https://www.amazon.com/Advanced-Solar-Distillation-Systems-Principles-Application/dp/9811046719.
13. Peng G, Sharshir SW, Hu Z, et al. (2021) A compact flat solar still with high performance. *Int J Heat Mass Transfer* 179: 121657. https://doi.org/10.1016/j.ijheatmasstransfer.2021.121657
14. Bhardwaj R, Ten Kortenaar MV, Mudde RF (2015) Maximized production of water by increasing area of condensation surface for solar distillation. *Appl Energy* 154: 480–490. https://doi.org/10.1016/j.apenergy.2015.05.060

15. Mohamed AF, Hegazi AA, Sultan GI, et al. (2019) Augmented heat and mass transfer effect on performance of a solar still using porous absorber: Experimental investigation and exergetic analysis. *Appl Therm Eng* 150: 1206–1215. https://doi.org/10.1016/j.applthermaleng.2019.01.070
16. Bataineh KM, Abbas MA (2020) Performance analysis of solar still integrated with internal reflectors and fins. *Sol Energy* 205: 22–36. https://doi.org/10.1016/j.solener.2020.04.059
17. Porta-Gándara MA, Fernández-Zayas JL, Chargoy-del-Valle N (2020) Solar still distillation enhancement through water surface perturbation. *Sol Energy* 196: 312–318. https://doi.org/10.1016/j.solener.2019.12.028
18. Jani HK, Modi KV (2019) Experimental performance evaluation of single basin dual slope solar still with circular and square cross-sectional hollow fins. *Sol Energy* 179: 186–194. https://doi.org/10.1016/j.solener.2018.12.054
19. Kabeel AE, Abdelgaied M (2020) Enhancement of pyramid-shaped solar stills performance using a high thermal conductivity absorber plate and cooling the glass cover. *Renewable Energy* 146: 769–775. https://doi.org/10.1016/j.renene.2019.07.020
20. Esfe MH, Esfandeh S, Toghraie D (2021) Optimization of influential geometrical parameters of single slope solar still equipped with thermoelectric system to achieve maximum desalinated water. *Energy Rep* 7: 5257–5268. https://doi.org/10.1016/j.egyr.2021.08.106
21. Esfe MH, Toghraie D (2022) Numerical study on the effect of solar radiation intensity on the fresh water productivity of solar still equipped with Thermoelectric Cooling System (TEC) for hot and dry areas of Semnan. *Case Stud Therm Eng* 32: 101848. https://doi.org/10.1016/j.csite.2022.101848
22. Sheikholeslami M, Said Z, Jafaryar M (2022) Hydrothermal analysis for a parabolic solar unit with wavy absorber pipe and nanofluid. *Renewable Energy* 188: 922–932. https://doi.org/10.1016/j.renene.2022.02.086
23. Abd Al-wahid WA, Saad HA, Hasan ZH, et al. (2022) Experimental study of the performance of hemispherical solar still with optimum value of rocks as heat transfer enhancers. *AIMS Energy* 10: 885–899. https://doi.org/10.3934/energy.2022040
24. Kabeel AE, Abdelgaied M, Mahmoud GM (2021) Performance evaluation of continuous solar still water desalination system. *J Therm Anal Calorim* 144: 907–916. https://doi.org/10.1007/s10973-020-09547-5
25. Park CD, Lim BJ, Chung KY, et al. (2016) Experimental evaluation of hybrid solar still using waste heat. *Desalination* 379: 1–9. https://doi.org/10.1016/j.desal.2015.10.004
26. Sohani A, Hoseinzadeh S, Samiezadeh S, et al. (2022) Machine learning prediction approach for dynamic performance modeling of an enhanced solar still desalination system. *J Therm Anal Calorim* 147: 3919–3930. https://doi.org/10.1007/s10973-021-10744-z
27. Tuly SS, Sarker MRI, Das BK, et al. (2021) Effects of design and operational parameters on the performance of a solar distillation system: A comprehensive review. *Groundwater Sustainable Dev* 14: 100599. https://doi.org/10.1016/j.gsd.2021.100599
28. Singh AK, Yadav RK, Mishra D, et al. (2020) Active solar distillation technology: A wide overview. *Desalination* 493: 114652. https://doi.org/10.1016/j.desal.2020.114652

29. Lee HS (2017) Thermoelectrics: Design and Materials, 1st ed., Mishigan: John Wiley & Sons. Available from: https://www.academia.edu/en/73566131/Thermoelectrics_Thermoelectrics_Design_and_Materials.
30. Riffat SB, Ma X (2003) Thermoelectrics: A review of present and potential applications. *Appl Therm Eng* 23: 913–935. https://doi.org/10.1016/S1359-4311(03)00012-7
31. Duan M, Sun H, Lin B, et al. (2021) Evaluation on the applicability of thermoelectric air cooling systems for buildings with thermoelectric material optimization. *Energy* 221: 119723. https://doi.org/10.1016/j.energy.2020.119723
32. Shen ZG, Tian LL, Liu X (2019) Automotive exhaust thermoelectric generators: Current status, challenges and future prospects. *Energy Convers Manage* 195: 1138–1173. https://doi.org/10.1016/j.enconman.2019.05.087
33. Liu Z, Li W, Zhang L, et al. (2019) Experimental study and performance analysis of solar-driven exhaust air thermoelectric heat pump recovery system. *Energy Build* 186: 46–55. https://doi.org/10.1016/j.enbuild.2019.01.017
34. Siddique ARM, Muresan H, Majid SH, et al. (2019) An adjustable closed-loop liquid-based thermoelectric electronic cooling system for variable load thermal management. *Therm Sci Eng Prog* 10: 245–252. https://doi.org/10.1016/j.tsep.2019.02.004
35. Liu W, Hu J, Zhang S, et al. (2017) New trends, strategies and opportunities in thermoelectric materials: A perspective. *Mater Today Phys* 1: 50–60. https://doi.org/10.1016/j.mtphys.2017.06.001
36. Phadatare MK, Verma SK (2007) Influence of water depth on internal heat and mass transfer in a plastic solar still. *Desalination* 217: 267–275. https://doi.org/10.1016/j.desal.2007.03.006
37. de Garayo SD, Martínez A, Aranguren P, et al. (2021) Prototype of an air to air thermoelectric heat pump integrated with a double flux mechanical ventilation system for passive houses. *Appl Therm Eng* 190: 116801. https://doi.org/10.1016/j.applthermaleng.2021.116801


AIMS Press